ELSEVIER

CrossMark

Oxidative coupling of methane: catalytic behaviour assessment via comprehensive microkinetic modelling

V.I. Alexiadis, J.W. Thybaut*, P.N. Kechagiopoulos, M. Chaar, A.C. Van Veen, M. Muhler, G.B. Marin

Laboratory for Chemical Technology, Ghent University, Technologiepark 914, B-9052 Zwijnaarde, Belgium

ARTICLE INFO

ABSTRACT

A comprehensive microkinetic model, including catalyst descriptors, that accounts for thermal, homogeneous and catalytic, heterogeneous reaction steps in the oxidative coupling of methane has been used in the assessment of kinetic data acquired on different catalysts. The applicability of the model was extended from alkali magnesia catalysts represented by Li/MgO and Sn–Li/MgO, to a new class of materials, namely alkaline earth-promoted lanthana catalysts, represented by Sr/La_2O_3. To simulate adequately the large experimental dataset, acquired with the latter catalyst, the surface reaction network of the microkinetic model was expanded. The resulting model succeeded in adequately simulating the C_2, that is, ethane and ethene, production, both individually and as a lump during regression. It was found that the activity of Sr/La_2O_3, in terms of methane conversion, is 33 and five times higher than that of Li/MgO and Sn–Li/MgO, respectively. This is attributed mainly to the higher stability of adsorbed hydroxyl, the higher stability of adsorbed oxygen, and the higher active density of Sr/La_2O_3. The selectivity toward C_2 products was found to depend on the methyl radical sticking coefficient and the stability of the adsorbed oxygen and was the highest on the Sn-promoted LiMgO catalyst, that is, 70% at about 5% methane conversion at 1023 K, 190 kPa, and inlet molar CH_4/O_2 ratio of 4.

© 2014 Elsevier B.V. All rights reserved.

1. Introduction

The oxidative coupling of methane (OCM) to C_2 and higher hydrocarbons has been widely accepted as a promising route to upgrade natural gas since the pioneering work of Keller and Bhasin in the early 80s [1]. Since then, several metal oxides have been proven to be effective OCM catalysts, such as Li/MgO and Sn-doped Li/MgO [2,3], Sr-promoted rare earth (La, Ce, Pr, Nd, etc.) catalysts [4], Na–Mn–W/SiO$_2$ [5–8], and Sn-, Zr-, P-, S-doped Na–Mn–W/SiO$_2$ catalysts [8–11]. However, none of them has reached the stage of commercial implementation yet, since their performance in terms of C_2 yield remains relatively low, despite all progress made.

High-throughput experimentation combined with combinatorial chemistry is capable of evaluating a large number of candidate catalysts in a short period of time. However, relating catalyst descriptors in the latter approach only to synthesis parameters prevents deepening the fundamental understanding of the reaction. It has been suggested [12–14] that a microkinetic analysis would be a valuable guiding technique in the search for new catalysts by combinatorial chemistry. Microkinetic analyses allow

accounting for the fundamental catalytic surface chemistry in a kinetic model in the form of elementary steps and catalytic cycles. Catalyst descriptors incorporated into such models are, in principle, measured independently or calculated applying theoretical chemistry. Catalyst descriptors correspond to a physical or chemical property of the catalyst in interaction with the reacting species and potentially affect the reaction kinetics via pre-exponential factors, activation energies, or reaction enthalpies. The incorporation of the catalyst descriptors can take place through the implementation of thermodynamic relationships, for example, Born Haber cycles or Polanyi relationships [13,14], the latter more specifically exploiting the chemical similarity between various catalytic elementary steps. Due to these catalyst descriptors, the kinetic behaviour of an entire catalyst family, and even of various catalyst families, rather than of a single catalyst can be evaluated by the microkinetic model. Consequently, optimized catalyst descriptor values can be determined and related to novel catalyst compositions and/or structures [13,14]. The actual synthesis of these microkinetic model-based catalysts is the challenge to be met to close the loop in rational catalyst design [12–14].

The above-described approach can be adopted in the case of OCM, which is a complex reaction in which catalytic and gas phase reactions interact with each other [15], as depicted in Fig. 1. This figure constitutes an elaborated version of a literature-reported figure

* Corresponding author. Tel.: +32 9 331 1752.
  E-mail address: Joris.Thybaut@UGent.be (J.W. Thybaut).

<div style="border:1px solid">

Nomenclature

Roman letters

b	the parameter vector containing the adjustable parameters
E_0	intrinsic activation barrier of a reaction family (kJ/mol)
$F_{reactants}$	flow rate of reactants ($CH_4 + O_2$) (mol/s)
p	pressure (kPa)
rf_i	reaction family i
S_i	selectivity toward product i (%)
T	temperature (K)
W	catalyst loading (kg)
X_i	conversion of reactant i (%)
y	observed molar fractions
$\hat{y}$	calculated molar fractions

Greek letters

α	transfer coefficient of a reaction family
ΔH	reaction enthalpy (kJ/mol)
$\sigma_{j,k}^{-1}$	element of the inverse of the error variance–covariance matrix

</div>

describing the OCM reaction [14]. The catalyst is activated through dissociative oxygen chemisorption and subsequently produces gas phase methyl radicals by hydrogen abstraction from methane. Methyl radicals can couple in the gas phase to form ethane, which in turn can be dehydrogenated into ethylene. However, they can also be oxidized toward undesired carbon oxides, CO, and CO_2, in the gas phase as well as by interaction with the catalyst surface [16].

In the work of Couwenberg et al. [3], it was established that gas phase radicals are highly reactive and lead to irreducible mass transport limitations. This effectively means that the pellet size necessary to consider the internal concentration gradients as negligible is so small that it would lead to an unacceptable pressure drop over the catalyst bed. As a result, these transport limitations have to be explicitly accounted for during the determination of OCM kinetics. A one-dimensional, heterogeneous reactor model was specifically developed by Couwenberg et al. [2,3] to properly describe the interaction between elementary catalytic steps and gas phase steps. Sun et al. [14] expanded the surface reaction network, introducing reversible reaction steps and elaborating on the deep oxidation steps. Additionally, catalyst descriptors were introduced in the model, so as to facilitate knowledge extraction from high-throughput experiments. Recently, in the work by Thybaut et al. [13], the surface reaction network was further elaborated, including reaction steps accounting for the heterogeneous oxidation of ethylene.
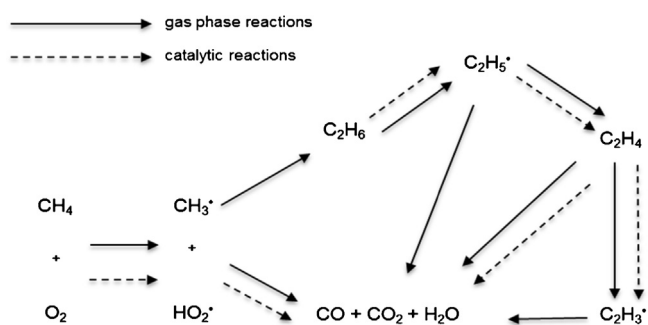

Fig. 1. Global reaction steps involved in OCM reaction, indicating their homogeneous and/or heterogeneous character.

Table 1
(**a**) Physical properties of the investigated catalysts.

Catalyst	Sr/La_2O_3	Li/MgO	Sn–Li/MgO
Surface area ($m^2\,kg_c^{-1}$)	2000	1000	2800
Porosity ($m_g^3\,m_c^{-3}$)	0.27	0.29	0.27
Density ($kg_c\,m_c^{-3}$)	2300	2350	2300

(**b**) Operating conditions employed over the investigated catalysts.

Operating conditions	Sr/La_2O_3	(Sn–)Li/MgO[*]
Pressure (kPa)	190	108–130
Temperature (K)	980–1180	947–1013
CH_4/O_2 ($mol_{CH_4}\,mol_{O_2}^{-1}$)	2–4	2–12
$W/F_{reactants}$ ($kg\,s\,mol^{-1}_{reactants}$)	0.2–1.2	2–12
N_2 dilution (%)	80	0
Radius of catalyst pellet (m)	1×10^{-4}	1.25×10^{-4}

[*]The experimentation has been reported previously [2,3].

In the current work, an enhanced version of the OCM microkinetic model [13] is presented, which aims at describing adequately large amounts of experimental data, produced over various catalyst families. The gas phase reaction network was adopted from Chen et al. [17], while the catalytic reaction network was enhanced compared to previous work [13] as elaborated in more detail in the recent work by Kechagiopoulos et al. [18]. The microkinetic model was incorporated into a one-dimensional heterogeneous reactor model. The overall model was employed to investigate the performance of catalysts, representative of two different catalyst families, that is, alkaline earth-promoted lanthana catalysts and alkali magnesia-based catalysts.

2. Procedures

2.1. Experimental

An extensive OCM experimental dataset was acquired over a Sr/La_2O_3 catalyst covering a wide range of operating conditions. A brief description is given of the Sr/La_2O_3 catalytic material, the experimental setup, and the employed operating conditions during the OCM experiments. Materials and procedures for the acquisition of literature data on Li/MgO and Sn–Li/MgO performances [2,3] are provided alongside for reference.

2.1.1. Catalyst

Alkaline earth-promoted La_2O_3 catalysts have been reported to be efficient catalytic materials in the OCM reaction [19,20]. Among these catalysts, the Sr-promoted ones have been found to exhibit superior performance in terms of activity as well as of selectivity to C_2 products. This has been attributed to the large number of strong basic sites and intermediate strength acid sites they contain [19]. Moreover, it was established that a low Sr to La ratio enhances the OCM activity and selectivity of the catalyst [19]. Hence, within the current study, the composition of the investigated catalyst was selected as 1wt% Sr/La_2O_3. Table 1a presents the main structural properties of this catalyst. The values correspond to the lined-out catalyst (see Section 2.1.3). The respective values for the MgO catalysts [14] are also shown in Table 1a. As can be easily observed, the investigated catalysts present similar physical properties. The low value of the surface area of Sr/La_2O_3 is in line with previous findings [19].

2.1.2. Setup

Experimental data for microkinetic model validation were acquired in a fixed bed reactor. Special attention was paid to operate the reactor in the plug-flow regime with minimal axial and radial temperature gradients and negligible pressure drop over the catalyst bed. The latter conditions justify the use of a one-dimensional